Fast Proton Spectroscopic Imaging Employing *k*-Space Weighting Achieved by Variable Repetition Times

Bernd Kühn, Wolfgang Dreher, David G. Norris, Dieter Leibfritz

A *k*-space weighted spectroscopic imaging (SI) method is presented that allows a reduction in the total data acquisition time by up to 55% compared with standard SI. The *k*-space weighting is achieved by varying the repetition time, thus realizing an inherent apodization that corresponds to a circularly symmetric generalized Hamming filter. The flip angle is varied with the repetition time to enhance the signal-to-noise ratio. These techniques were employed using a short echo time of 10 ms. *In vivo* measurements on healthy rat brain at 4.7 T were conducted, obtaining two-dimensional spectroscopic imaging data from a 25 × 25 circularly reduced *k*-space area in as little as 5 min. The signal-to-noise ratio is sufficiently high to detect *J*-coupled resonances such as *myo*-inositol or glutamate/glutamine, demonstrating the ability to combine short acquisition times with comprehensive metabolic information. The T_1 dependency of the apodization and the corresponding point spread function was evaluated by computer simulations. The achievable signal-to-noise ratio per unit time was compared with standard SI giving a parameter-dependent advantage of approximately 20% of the standard SI method.

Key words: proton spectroscopic imaging; *k*-space weighting; rat brain.

INTRODUCTION

Long total data acquisition times are a severe limitation of standard spectroscopic imaging (SI, 1, 2). Acceptable total examination times, in human as well as animal studies, force a compromise between spatial resolution and the number of spatial dimensions. As a consequence, SI examinations very often have to be restricted to a single slice (3–5) or, using a multislice technique (6–9), to a few noncontiguous slices. A full 3-dimensional SI examination that does not exceed tolerable measurement durations is only possible at the expense of a distinctly reduced in-plane spatial resolution. Further problems may arise from motion artifacts, which corrupt the localization and diminish the signal-to-noise ratio (SNR), because the risk of irregular subject movement increases with the duration of the examination.

To overcome these limitations of standard SI, different methods have been used to shorten the duration of the experiment. One strategy is to use a multiecho technique acquiring several points in *k*-space per signal excitation (8, 10–13). These techniques give a distinct reduction in data acquisition time. Unfortunately, it is difficult to detect short T_2 and/or *J*-coupled metabolites with a good spectral quality using these techniques, and so the spectral information is mainly limited to the metabolites creatine/phosphocreatine (Cr/PCr), choline containing compounds (Cho), *N*-acetyl aspartate (NAA), and lactate.

An alternative approach, to significantly reduce the total measurement time uses a weighted *k*-space technique (14), either employing a variable number of accumulations or a variable repetition time. This technique has been successfully used in magnetic resonance imaging (15–18). In view of the limitations in SI, *k*-space weighting has the potential to enhance the usefulness of this NMR method in *in vivo* applications. In addition to a saving in data acquisition time, *k*-space weighting can be combined with short echo times leading to a reduction in signal losses due to T_2 relaxation and *J*-coupling. This combines short total data acquisition times and comprehensive metabolic information including *J*-coupled metabolites. Furthermore, short echo times give an additional contribution to the reduction in the acquisition time because it minimizes the number of averages required for a given SNR. Previous work using *k*-space weighting was performed by Hugg *et al.* (19) in phosphorous SI where the *k*-space weighting has been achieved by varying the number of averages per *k*-space coordinate.

In this study, the weighted *k*-space technique using a variable repetition time has been used for proton short echo time SI. *In vivo* studies on healthy rat brain prove the feasibility of detecting short T_2 and/or *J*-coupled metabolites in combination with short total data acquisition times. The influence of the variable repetition time on localization as well as the achievable SNR per unit time are discussed.

METHOD

k-Space Weighting and Apodization

The *k*-space weighting can be performed by employing either a variable number of averages or a variable repetition time. The use of a variable number of averages has two limitations: It is not possible to realize extremely short data acquisition times because a multiple acquisition of the central *k*-space points is required. Furthermore, the technique results in a coarse and terraced weighting function that may cause artifacts in the spatial domain. To prevent these artifacts additional postprocessing procedures may be necessary to correct the discontinuities in the weighting function. The method presented in this study circumvents these disadvantages by using variable repetition times. This technique reduces the minimum number of accumulations to one, yielding very short total data acquisition times and making a

MRM 35:457–464 (1996)

From the Universität Bremen, Bremen, Federal Republic of Germany.

Address correspondence to: Dieter Leibfritz, Ph.D., Universität Bremen, FB 2, NW 2, Leobenerstr., 28334 Bremen, FRG.

Received April 20, 1995; revised November 17, 1995; accepted November 24, 1995.

0740-3194/96 $3.00

continuous weighting function possible. The central points in k-space are sampled with long repetition times to ensure a high SNR, while the outer points in k-space are sampled with shorter repetition times. To minimize signal fluctuations that may result from large changes in the repetition time, TR, this is steadily reduced throughout the experiment. This is achieved by a k-space sampling scheme that differs from the frequently used line-oriented scheme and starts from the center. The k-space is sampled in concentric circles with increasing radii k_r with

$$k_r = \sqrt{k_x^2 + k_y^2}, \quad [1]$$

where k_x and k_y are the coordinates in k-space. The repetition delay is reduced with increasing distance from the center of k-space. This results in an apodization in k-space that can replace an apodization by postprocessing. In this study an apodization function with rotational symmetry is employed

$$a = a(k_r), \quad [2]$$

corresponding to the symmetry of the k-space sampling scheme. The apodization function is related to the transverse magnetization, M_{xy}, by:

$$a(k_r) = \frac{M_{xy}(TR(k_r), T_1, \theta)}{M_{xy}(TR(k_r = 0), T_1, \theta)}, \quad [3]$$

where T_1 is the longitudinal relaxation time, θ is the flip angle and $M_{xy}(TR(k_r = 0), T_1, \theta)$ is the transverse magnetization measured at the k-space center. Under the assumption that the changes in TR are small enough, M_{xy} can be calculated to a good approximation from the equation holding for the dynamic equilibrium. In the case of a spin-echo sequence where the time between the excitation and refocusing pulse is short in relation to T_1 and where the excitation pulse is directly preceded by an inversion pulse this quantity is given by

$$M_{xy}(\tau, \theta) = M_0 \frac{1 - \exp(-\tau)}{1 - \cos\theta \cdot \exp(-\tau)} \sin\theta, \quad [4]$$

where M_0 is the longitudinal magnetization in thermal equilibrium and $\tau = TR/T_1$. In the derivation of Eq. [4], the assumption is made that no transverse magnetization is present at the end of the relaxation delay; i.e., that it has either completely decayed due to T_2 relaxation or that it has been dephased by a gradient.

For a given flip angle, θ, Eqs. [3] and [4] are combined to give the repetition time as a function of k_r:

$$TR(k_r) = -T_1 \cdot \ln\left(\frac{\tilde{M}_{xy}(\tau(k_r = 0), \theta) \cdot a(k_r) - \sin\theta}{\tilde{M}_{xy}(\tau(k_r = 0), \theta) \cdot a(k_r) \cdot \cos\theta - \sin\theta}\right), \quad [5]$$

with

$$\tilde{M}_{xy}(\tau, \theta) = \frac{M_{xy}(\tau, \theta)}{M_0}. \quad [6]$$

This equation holds for a flip angle that is fixed for all phase encoding steps. To enhance the SNR it is sensible to use a flip angle that varies in accordance with the repetition time. The flip angle, θ_{opt}, giving the highest transverse magnetization has to be calculated for each individual repetition time. With the same assumptions that have been used in connection with Eq. [4], the relation between θ_{opt} and the repetition time is given by the Ernst-equation:

$$\cos\theta_{opt} = \exp(-\tau). \quad [7]$$

For a variable flip angle, Eq. [5] has to be rewritten as:

$$TR(k_r) = -T_1 \cdot \ln\left(\frac{\tilde{M}_{xy}(\tau(k_r = 0), \theta(k_r = 0)) \cdot a(k_r) - \sin\theta(k_r)}{\tilde{M}_{xy}(\tau(k_r = 0), \theta(k_r = 0)) \cdot a(k_r) \cdot \cos\theta(k_r) - \sin\theta(k_r)}\right). \quad [8]$$

The repetition time and the flip angle can be calculated as a function of k_r by iteration of Eqs. [7] and [8]. An alternative approach to determine the repetition time is given in the appendix.

Signal-to-noise Ratio per Unit Time

An important parameter of SI is its performance in terms of the SNR achieved per unit time (SNR_t). In a comparison between standard and k-space weighted SI, identical experimental conditions can be assumed. As a consequence, the root mean square of the noise amplitude of the individual phase encoded NMR signals will be equal for both methods. Hence, the SNR_ts can be compared by considering only the transverse magnetization and the total data acquisition time

$$\frac{(SNR_t)_{STD}}{(SNR_t)_{WK}} = \frac{\left(\sum_{n=1}^{N} M_{xy}(\tau_n, \theta_n)\Big/\sqrt{\sum_{n=1}^{N} TR_n}\right)_{STD}}{\left(\sum_{n=1}^{N} M_{xy}(\tau_n, \theta_n)\Big/\sqrt{\sum_{n=1}^{N} TR_n}\right)_{WK}}, \quad [9]$$

where the indices STD denote standard SI and WK the weighted k-space SI method. Both methods are assumed to acquire N individually phase-encoded time domain signals that give the entire transverse magnetization $\Sigma_{n=1}^{N} M_{xy}(\tau_n, \theta_n) \cdot \tau_n$ and θ_n are the repetition time divided by T_1 and the flip angle of the nth phase-encoded signal. By analogy, $\Sigma_{n=1}^{N} TR_n$ is the total data acquisition time of an SI experiment.

EXPERIMENTAL

All experiments were performed on a 4.7 T/40 cm Biospec system (Bruker, Karlsruhe, FRG) equipped with self-shielded gradients (Magnex, Abingdon, UK) capable of switching 150 mT/m in 500 μs. Phantom experiments were conducted using a saddle-shaped volume coil for RF transmission and signal reception. In *in vivo* studies the volume coil was employed for RF transmission only whereas an 18-mm actively decoupled surface coil was used for signal reception.

The pulse sequence that was used in this study is shown in Fig. 1. The echo time was 10 ms. An outer volume suppression was employed to reduce strong wa-

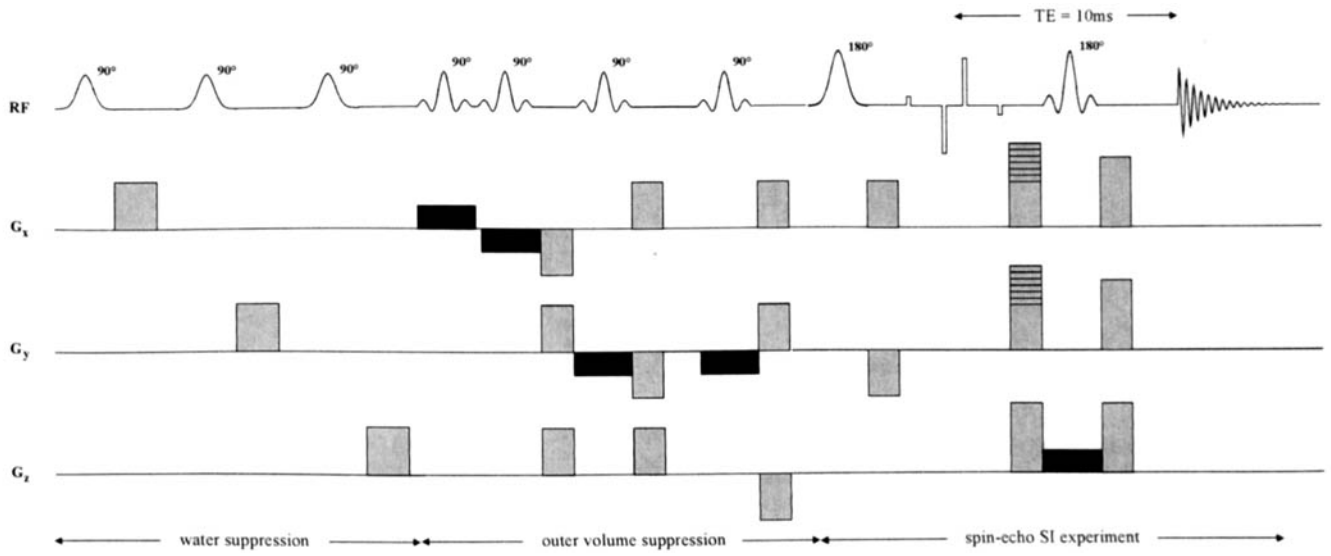

FIG. 1. *k*-Space weighted SI pulse sequence (not to scale). The pulse sequence is arranged in three parts: water suppression by three Gaussian pulses, outer volume suppression and the spin-echo SI experiment with an echo time of 10 ms.

ter and fat signals that may arise from regions surrounding the brain. The outer volume suppression scheme has been adapted to the experimental situation as follows: The region nearest the surface coil, on top of the rat's head, gave rise to the most interfering signals, therefore this was presaturated by two consecutive RF-pulses, each followed by a dephasing gradient, whereas the lateral regions were presaturated by only one pulse. Water suppression was conducted by three Gaussian pulses of 15 ms duration, each followed by spoiler gradients in the *x*-, *y*-, and *z*-direction. The total duration of this preparation period consisting of outer volume and water suppression was 105 ms. Suppression of the water signal by Gaussian pulses was combined with a frequency selective excitation using a $1\text{–}2\tau\text{-}5.4\text{-}\tau\text{-}\overline{5.4}\text{–}2\tau\text{-}\overline{1}$ hard pulse sequence (20). The interpulse delay, τ, was equal to 1.25 ms, giving a frequency difference between neighboring excitation nulls of 800 Hz. This hard pulse sequence has been optimized for a flip angle of 79.2° to give excellent excitation characteristics (20) whereas flip angles varying between 40° and 70° were used in this study. This led to a loss in the uniformity of the plateau of the excitation band, but these variations do not exceed 15%. A nonselective adiabatic inversion pulse (21) was directly applied before the excitation pulse to offset the effect of the 180° refocusing pulse on the longitudinal relaxation. This ensured that the flip angles, required for the maximum signal strength in dynamic equilibrium, were smaller than 90°. An optimized four zero sinc pulse (22) was employed slice selectively to refocus transverse magnetization from a coronal section of the rat brain. Phase encoding was conducted on a circularly reduced *k*-space (23) with a 25-point diameter. The apodization function applied in this study was a circularly symmetric generalized Hamming filter:

$$a(k_r) = \alpha + (1 - \alpha)\cos\left(\frac{\pi k_r}{k_{r,\max}}\right), \qquad [10]$$

where $k_{r,\max}$ is the radius of the circularly reduced *k*-space and α is the apodization parameter. The calculation of $TR(k_r)$ and $\theta_{opt}(k_r)$ was started in the center of *k*-space and was proceeded with increasing k_r. The central point was acquired with a repetition delay of 1500 ms and a flip angle calculated from Eq. [7]. A longitudinal relaxation time of 1500 ms has been assumed as an approximation to the T_1 values of Cr/PCr, Cho, and NAA at 4.7 T as described below. All succeeding values of $TR(k_r)$, $\theta_{opt}(k_r)$ were iteratively calculated from Eqs. [7] and [8] using the preceding values as a starting point for the iteration. The parameter α of the generalized Hamming function has been chosen to be 0.75. This corresponds to a minimum value of the apodization function of 0.5. A lower value of α would require a *TR* shorter than the minimum repetition time of the pulse sequence. The rotational symmetry of the employed *k*-space filter implies that the repetition times and flip angles are equal for all *k*-space points having the same radius. This would give discontinuities in *TR* and θ_{opt} whenever the acquisition proceeded from one radius in *k*-space to the next and may cause localization artifacts because the magnetization will not immediately return to its dynamic equilibrium value at the new *k*-space radius. These artifacts can be prevented if the values of *TR* and θ_{opt} belonging to one radius are modified to realize a smooth transition to the next radius. Equations [7] and [8] were used to calculate *TR* and θ_{opt} for each *k*-space radius. The polar coordinate (k_r,ϕ) of each phase-encoding step in *k*-space was calculated and the experimental order determined on the basis of increasing coordinate value; i.e., the phase-encoding steps with the smallest k_r values were executed first, and within groups of equal k_r the lowest ϕ values were first applied. *TR* as a function of experiment number is plotted in Fig. 2. The *TR* values were corrected by connecting the points at each k_r value that had the highest ϕ value and increasing *TR* for all other ϕ values to lie on the connecting line as shown in Fig. 2. This modification introduces a minor deviation of the apodization function from rotational symmetry. The use of only one accumulation gave a total data acquisition time of 5 min for the apodization parameter α = 0.75. Begin-

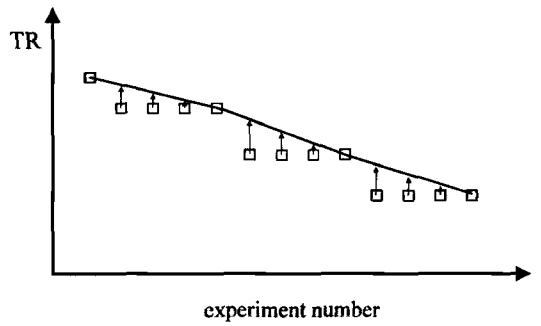

FIG. 2. Modification of the calculated repetition time (open squares) to realize a smooth decline of these quantity (figure is not to scale). The polar coordinate (k_r, ϕ) of each phase-encoding step in k-space was calculated and the experimental order determined on the basis of increasing coordinate value, i.e., the phase-encoding steps with the smallest k_r values were executed first, and within groups of equal k_r the lowest ϕ-values were first applied. The *TR* values were increased to lie on the connecting line as indicated by the vertical arrows.

ning from the echo maximum, 512 points were acquired in the time domain within 128 ms using a sweep width of 2000 Hz. The second half of the NMR signal was replaced by a series of zeroes to enhance the SNR. The data were reconstructed on a 32 × 32 × 512 matrix. No additional k-space filtering was applied by postprocessing. To reduce Gibbs ringing artifacts, the time domain data were multiplied with a decaying exponential, that gives a line broadening of 2 Hz. A field of view of (32 × 32) mm^2 and a slice thickness of 3 mm gave a nominal voxel size of 3 μl.

In vivo studies were conducted on male Wistar rats of 250–300 g body weight. The animals were anesthetized with 0.8–1.5% halothane in a mixture of N_2O/O_2 (70/30%).

RESULTS

Technical Verification

The reproducibility of the Hamming apodization by variable repetition times was examined on a spherical water-filled phantom of 3.9 cm diameter. The repetition times were calculated from the T_1 value of the phantom (T_1 = 2700 ± 50 ms). Figure 3 presents the calculated generalized Hamming function (α = 0.75, solid line) and the measured signal intensities (open squares) as a function of the radius in k-space. Each point represents the signal intensity obtained with a single acquisition at the corresponding k_r. The shape of the generalized Hamming filter is almost exactly reproduced. The fluctuations of the signal intensities are mainly due to instrumental instabilities. This is demonstrated by the signal intensities of a standard SI measurement (open circles) as presented in Fig. 3. These results indicate that the changes in *TR* and θ_{opt} between two consecutive phase-encoding steps are small enough to keep the spin system near its dynamic equilibrium, avoiding additional signal fluctuations that may corrupt localization. This justifies the use of Eqs. [4] and [7], which are based on the assumption that the spin system is in dynamic equilibrium.

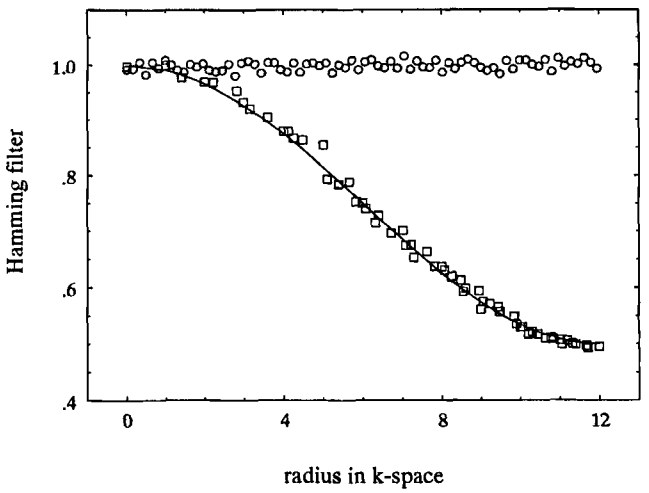

FIG. 3. Comparison of the calculated generalized Hamming filter (α = 0.75, solid line) and the experimental signal intensities in a variable repetition time SI experiment (open squares) measured on a water filled spherical phantom. The signal intensities of a standard SI experiment using a constant *TR* (open circles) demonstrate the signal fluctuations that are due to experimental instabilities.

The T_1 values of the main metabolites Cr/PCr, Cho, and NAA were estimated in a healthy rat brain to choose a suitable T_1 value as a basis for the calculation of the repetition times *in vivo*. An inversion recovery double spin-echo sequence with an echo time of 136 ms and a repetition time of 10 s was used to acquire fully relaxed spectra from a (3 × 3 × 3) mm^3 voxel located in the striatum of the brain. Ten different inversion times, TI, covering a range from 100 to 7000 ms, were applied. The signal intensities, S(TI), obtained from the metabolites were fitted by

$$S(\mathrm{TI}) = S_0\left(1 - 2\exp\left(-\frac{\mathrm{TI}}{T_1}\right)\right). \qquad [11]$$

S_0 is a constant that depends on the longitudinal magnetization in thermal equilibrium and echo time. The analysis of the experimental data gave a longitudinal relaxation time of (1450 ± 150) ms for Cho, (1350 ± 150) ms for Cr/PCr, and (1650 ± 150) ms for NAA. Based on these results, a T_1 value of 1500 ms was used to calculate the repetition times for the *in vivo* experiments. Taking into account the uncertainty in the experimentally determined values, the T_1 times of the metabolites may differ by up to 300 ms from the value chosen. These differences may be increased by variations in T_1 between different parts of the brain and between different animals.

It is important to evaluate the susceptibility of k-space weighting by variable repetition times to these variations in T_1 because they may cause differences in apodization and hence in the spatial localization of the various metabolites. Computer simulations were conducted to calculate the shape of the k-space filter and the corresponding point spread function (PSF) if the T_1 value of the metabolite deviates from the assumed T_1 value of 1500 ms. Figure 4 presents the cross sections of the k-space filter for T_1 values of 500 ms (solid line) and 2500 ms (dashed line). The repetition times and the optimized flip

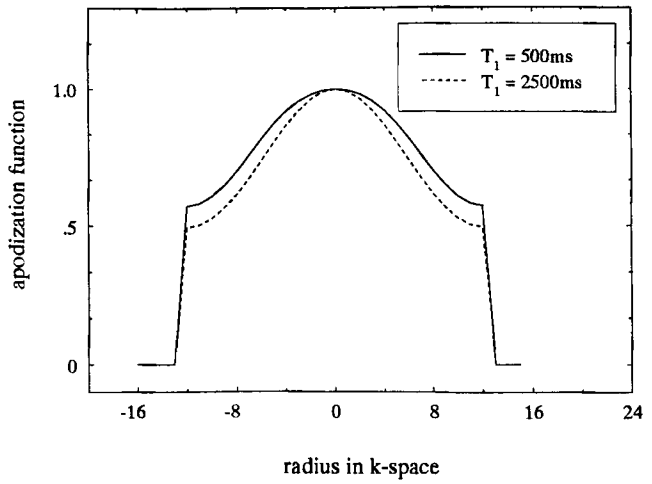

FIG. 4. Simulated *k*-space filter demonstrating the low T_1 dependency of the apodization by variable repetition times. The repetition times were calculated to achieve a circularly symmetric Hamming filter (α = 0.75) assuming a T_1 value of 1500 ms. The simulations were conducted for metabolites with T_1 values of 500 ms (solid line) and 2500 ms (dashed line). The flip angle was varied corresponding to Eq. [7] using a T_1 value of 1500 ms.

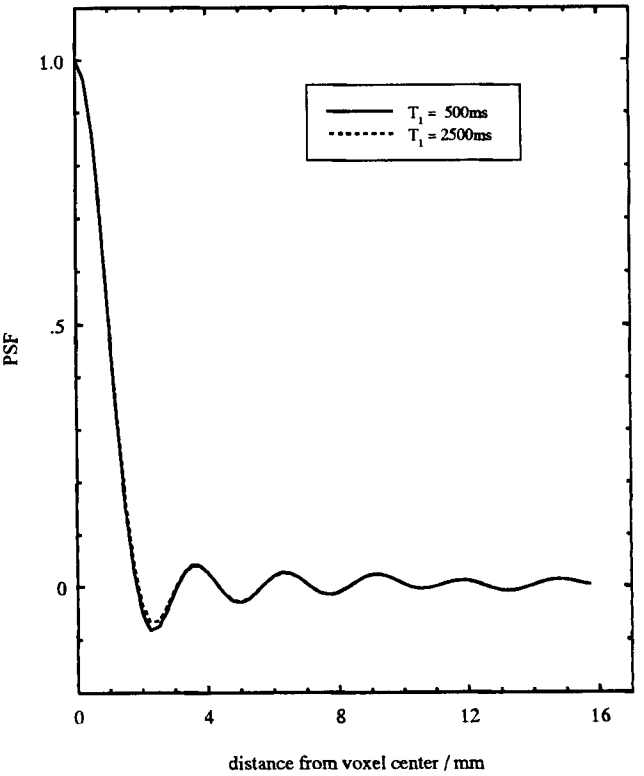

FIG. 5. Simulation of the point spread functions from point sources with 500 and 2500 ms longitudinal relaxation times. The flip angle used in this simulation was varied with the repetition time (Eq. [7]). Circularly reduced *k*-space sampling with a diameter of 25 points was used. The field-of-view was 32 mm.

angles have been determined for a T_1 value of 1500 ms. Despite these huge deviations in T_1, there are only small variations between the shapes of the normalized filter functions and between the declines from the center to the edges: In the case of T_1 = 500 ms, the filter function drops to 0.57 while it falls to 0.49 in case of T_1 = 2500 ms. A value of 0.5 is expected for α = 0.75. The small deviations in the *k*-space filter are reflected in the corresponding PSFs (Fig. 5) that are very similar for both T_1 times. The insensitivity of the filter function is a consequence of the employment of variable flip angles. This can be understood by considering the two extreme cases $T_1 \ll TR(k_r = 0)$ and $T_1 \gg TR(k_r = 0)$. A simulation of the shapes of the *k*-space filter using the same parameters as above with the exception of the flip angle that is assumed to be constant for all phase encoding steps will reveal almost no apodization for $T_1 \ll TR(k_r = 0)$ and a strong apodization for $T_1 \gg TR(k_r = 0)$. The application of a variable flip angle that is calculated, depending on the particular repetition time, from a T_1 value of 1500 ms will reduce these deviations in apodization. The signal strength in case of $T_1 \ll TR(k_r = 0)$ is mainly influenced by the flip angle and only to a marginally extend by the T_1 relaxation. The employment of a variable flip angle that is declining with increasing radius in *k*-space will therefore enhance the degree of apodization. The opposite is true for $T_1 \gg TR(k_r = 0)$. The signal strength is dominated by the partial saturation resulting in a strong signal drop for short repetition times. Application of variable flip angles reduce the partial saturation effect because the flip angle and the repetition time decrease with increasing radius.

It is important to compare the sensitivity of standard SI with *k*-space weighted SI to evaluate the potential of this fast SI method for *in vivo* applications. It was assumed that both experiments acquire a circularly reduced *k*-space with a 25-point diameter. Variable repetition time SI was supposed to use a repetition time that is 1500 ms in the center of *k*-space, declining to 350 ms at the edge of the sampled *k*-space area (α = 0.75, T_1 = 1500 ms). Standard SI is assumed to use a constant repetition time of 1500 ms. The flip angle is optimized in both cases to give the maximum signal intensity in dynamic equilibrium (Eq. [7]). The experimental conditions have to be the same for both methods to ensure the equality of the root mean square of the noise amplitudes. With this assumption Eq. [9] can be used to evaluate the SNR_t. If no apodization is applied by postprocessing, the SNR_t for the variable repetition time SI method is marginally lower, 3%, than for standard SI. To experimentally verify this result, standard SI and *k*-space-weighted SI measurements were conducted on a spherical phantom filled with a 100-m*M* aqueous alanine solution. The acquired spectra revealed almost no differences in the SNR_ts of both methods confirming the calculated values. In the previous comparison *k*-space-weighted SI has a poorer spatial resolution than standard SI because of its inherent apodization. To realize an identical spatial resolution for both methods, one has to apply the same apodization to the standard SI data by postprocessing, that has inherently been applied to the variable repetition time SI data during *k*-space sampling. To evaluate the effect of apodization on the SNR, the standard SI data from the phantom measurement were used. The comparison of the SNR_t of the non-apodized and the apodized (α = 0.75) standard SI data set revealed an increase in SNR of about

20% due to apodization. This increases the advantage of standard SI in SNR_t to 23%. This result holds for the specific parameters that have been used in this study. Variations in T_1, α or the repetition time, employed either for standard SI or for the central k-space point of variable repetition time SI, may alter this result.

In Vivo Application

Figure 6 shows phased spectra obtained from a voxel located in the cortex of a healthy rat brain. The data were acquired with standard SI (TR = 1500 ms) and the variable repetition time SI method for comparison. One accumulation gave total data acquisition times of 11 and 5 min, respectively. Both spectra present the main metabolite resonances assigned to Cho (3.22 ppm), Cr/PCr (3.04 ppm), and NAA (2.02 ppm). In addition, there are some minor resonances: Cr/PCr (3.93 ppm); glutamate, glutamine (Glx, 3.8 ppm); *myo*-inositol (Ins, 3.54 ppm); glucose (Glc), taurine (Tau) (3.4 ppm); NAA (2.70 ppm); glutamate, glutamine, GABA (2.2–2.4 ppm). The assignment of the metabolites has previously been given (24, 25). The spectrum obtained with the variable repetition time SI method shows no apparent differences in the signal intensities of metabolites compared with the standard SI data. Minor deviations between the spectra are within the limits of the experimental accuracy achievable with short echo time SI. Both spectra are in good agreement with results from other studies at 4.7 T where healthy rat brain was examined by short echo time SI with constant repetition time (26) or with short echo time single voxel spectroscopy (27). Figure 6 demonstrates the possibility of combining very short acquisition times with comprehensive metabolic information. The SNR achieved is sufficiently high to detect metabolites such as glutamate/glutamine or *myo*-inositol. Figure 7 presents a (3 × 3) matrix of spectra from a coronal slice of a healthy rat brain, acquired within 5 min. The decrease in SNR that is observed in proceeding from the top line to the bottom line of the matrix of spectra is due to the characteristic of the surface coil.

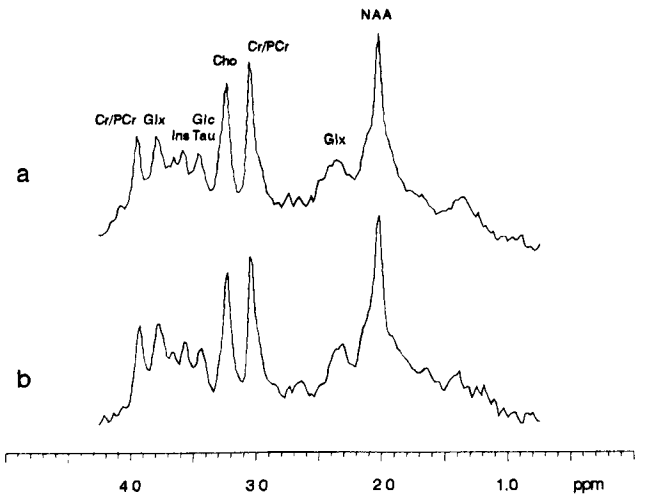

FIG. 6. Phased spectra from a voxel located in the cortex of a healthy rat brain acquired (a) with standard SI (constant repetition time, TR = 1500 ms) and (b) with the variable repetition time SI method (α = 0.75 ms, TR varies from 1500 ms in the center of k-space to 350 ms at the edge of the sampled k-space area). One accumulation gave a data acquisition time of 11 min for standard SI and 5 min for k-space weighted SI. The echo time was 10 ms.

DISCUSSION

The k-space sampling scheme employed distinctly reduces the duration of the measurement in comparison with standard SI. It has been demonstrated in this study that a saving in data acquisition time of up to 55% can be achieved in 2-dimensional (2D) SI depending on the chosen degree of apodization. This gives more flexibility in *in vivo* studies: The data acquisition time used for SI may be reduced to enhance the temporal resolution or to employ supplemental NMR imaging techniques that provide additional information. The application of k-space weighting by variable repetition times to 3-dimensional (3D) SI reduces the data acquisition time even more than in 2D SI. This is because the ratio of the number of acquisitions with long repetition times to the number of acquisition with short repetition times is significantly smaller for 3D SI than for 2D SI.

Although k-space weighting by variable repetition times may also be used with long echo times such as 136 or 272 ms, it is more reasonable to combine this technique with short echo times. This reduces signal losses due to T_2 relaxation and achieves the optimum reduction in total data acquisition time. Correspondingly, signal sacrifice due to J-coupling is minimized enabling the detection of J-coupled metabolites despite the short total data acquisition time.

It is important to notice that the T_1 weighting of the spectra acquired with the variable repetition time SI method is primarily determined by the repetition time of the central point in k-space. The decline in the repetition time, used to achieve an apodization, does only weakly effect the T_1 weighting of the spectra. This is a consequence of the minor T_1 dependency of the apodization function. Therefore, no substantial problems in the quantification of the spectra are introduced by variable repetition time SI.

The method presented is less sensitive to irregular movements of the examined subject compared with standard SI. This is a consequence of the shorter duration of the measurement, that diminishes the risk of the occurrence of movements during the study. In addition, the variable repetition time SI method, as presented in this study, does not employ a line-oriented k-space sampling scheme. The k-space sampling starts in the center, proceeding in concentric circles of increasing radii. The time required to sample the low spatial frequency components in k-space, which significantly influence the quality of the experimental results, is reduced in comparison with a line-oriented sampling scheme.

The k-space weighting by variable repetition times reveals a weak inherent T_1 dependency of the k-space filter function. To reduce this influence on localization, it is important to use variable flip angles that ensure a maximum signal intensity in dynamic equilibrium. The use of this technique results in very similar PSFs for the different brain metabolites. Because the differences in the PSF

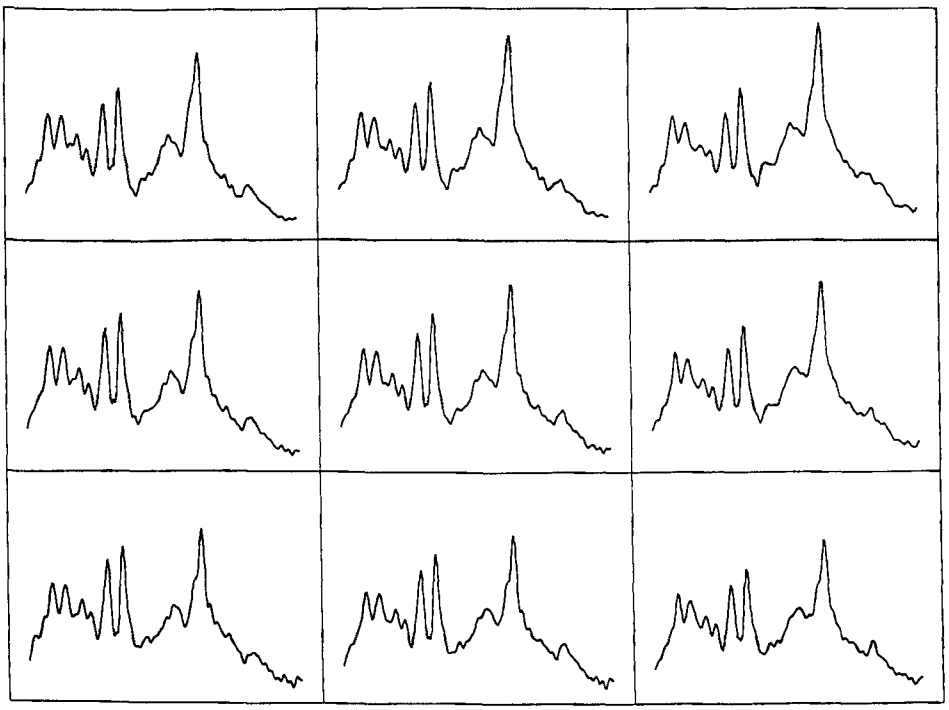

FIG. 7. Matrix of magnitude spectra from a coronal section of a healthy rat brain (*TE* = 10 ms). The spectra presented cover the range from 4 to 1 ppm. The data were acquired within 5 min using the variable repetition time method. The second half of the time domain data was replaced by zeroes. Each voxel represents a nominal volume of 3 μl.

for a T_1 of 500 ms and for a T_1 of 2500 ms are only minor, it is possible to use variable repetition time SI for the examination of brain diseases that are accompanied by changes in T_1 without severe consequences to the quality of localization of the metabolites. More severe drawbacks are the lower SNR_t in comparison with standard SI, and less flexibility in the degree of apodization because the *minimum* level is fixed before the measurement.

The *k*-space-weighted SI employing variable repetition times is a useful alternative to multiecho SI techniques. Although the latter methods can give shorter data acquisition times in 2D examinations, this advantage is less prominent in 3D measurements. There is also the fact that *k*-space-weighted SI makes significantly lower demands on the instrumentation. This may be of particular importance for applications using whole-body systems. Thus, the decision whether to use multiecho or *k*-space-weighted SI depends on the individual requirements such as the total data acquisition time, choice of the investigated metabolites, instrumentation, and number of spatial dimensions.

APPENDIX

As an alternative to the iterative calculation of the repetition time and the flip angle using Eqs. [7] and [8], *TR* can be determined by:

$$TR(k_r) = -T_1 \ln\left(\frac{1 + \exp(-\tau(k_r = 0)) - a(k_r)^2[1 - \exp(-\tau(k_r = 0))]}{1 + \exp(-\tau(k_r = 0)) + a(k_r)^2[1 - \exp(-\tau(k_r = 0))]}\right),$$

which can be derived from Eqs. [3], [4], and [7].

ACKNOWLEDGMENTS

The authors thank the referee who proposed the alternative approach to determine the repetition times in a *k*-space-weighted SI experiment by Eq. [12].

REFERENCES

1. T. R. Brown, B. M. Kincaid, K. Uğurbil, NMR chemical shift imaging in three dimensions. *Proc. Natl. Acad. Sci. USA* **79**, 3523–3526 (1982).
2. A. A. Maudsley, S. K. Hilal, W. H. Perman, H. E. Simon, Spatially resolved high resolution spectroscopy by "four-dimensional" NMR. *J. Magn. Reson.* **51**, 147–152 (1983).
3. C. T. W. Moonen, G. Sobering, P. C. M. van Zijl, J. Gillen, M. von Kienlin, A. Bizzi, Proton spectroscopic imaging of human brain. *J. Magn. Reson.* **98**, 556–575 (1992).
4. J. H. Duijn, G. B. Matson, A. A. Maudsley, J. W. Hugg, M. W. Weiner, Human brain infarction: proton MR spectroscopy. *Radiology* **183**, 711–718 (1992).
5. S. Posse, B. Schuknecht, M. E. Smith, P. C. M. van Zijl, N. Herschkowitz, C. T. W. Moonen, Short echo time proton MR spectroscopic imaging. *J. Comput. Assist. Tomogr.* **17**, 1–14 (1993).
6. J. H. Duyn, J. Gillen, G. Sobering, P. C. M. van Zijl, C. T. W. Moonen, Multisection proton MR spectroscopic imaging of the brain. *Radiology* **188**, 277–282 (1993).
7. D. Spielman, J. M. Pauly, A. Macovski, G. Glover, D. R. Enzmann, Lipid-suppressed single- and multisection proton spectroscopic imaging of the human brain. *J. Magn. Reson. Imaging* **2**, 253–262 (1992).
8. J. H. Duyn, C. T. W. Moonen, Fast proton spectroscopic imaging of human brain using multiple spin-echoes. *Magn. Reson. Med.* **30**, 409–414 (1993).
9. W. Dreher, D. Leibfritz, Double-echo multislice proton spectroscopic imaging using Hadamard slice encoding. *Magn. Reson. Med.* **31**, 596–600 (1994).
10. P. Mansfield, Spatial mapping of the chemical shift in NMR. *Magn. Reson. Med.* **1**, 370–386 (1984).
11. A. R. Guimaraes, J. R. Baker, R. M. Weisskoff, B. R. Rosen, R. G. Gonzalez, Echo planar metabolic imaging of brain, *in* "Proc., SMRM, 12th Annual Meeting, New York, 1993," p. 43.
12. D. G. Norris, W. Dreher, Fast proton spectroscopic imaging using the sliced *k*-space method. *Magn. Reson. Med.* **30**, 641–645 (1993).
13. S. Posse, C. De Carli, D. Le Bihan, Three-dimensional echo-

planar MR spectroscopic imaging at short echo times in the human brain. *Radiology* **192,** 733–738 (1994).
14. T. H. Mareci, H. R. Brooker, Essential considerations for spectral localization using indirect gradient encoding of spatial information. *J. Magn. Reson.* **92,** 229–246 (1991).
15. D. L. Parker, G. T. Gullenberg, P. R. Frederick, Gibbs artifact removal in magnetic resonance imaging. *Med. Phys.* **14,** 640 (1987).
16. R. K. Butts, F. Farzaneh, S. J. Riederer, J. N. Rydberg, R. C. Grimm, T_2-weighted spin-echo pulse sequence with variable repetition and echo times for reduction of MR image acquisition time. *Radiology* **180,** 551–556 (1991).
17. H. W. Korin, S. J. Riederer, J. P. Felmlee, A. E. Holsinger, R. L. Ehman, Improved efficiency in three-dimensional MR imaging through dynamic modification of repetition time, *in* "Proc., SMRM, 10th Annual Meeting, San Francisco, 1991," p. 273.
18. L. D. Mattinger, L. L. Shen, G. W. Mattinger, H. Chang, C. Yao, S. C. Chiang, R. S. Wagner, J. M. Coleman, D. M. Kramer, Performance optimization of mixed TR sequences, *in* "Proc., SMRM, 11th Annual Meeting, Berlin, 1992," p. 886.
19. J. W. Hugg, A. A. Maudsley, M. W. Weiner, G. B. Matson, Reduced voxel size and contamination in ^{31}P MR spectroscopic imaging, *in* "Proc., SMRM, 11th Annual Meeting, Berlin, 1992," p. 3813.
20. Z. Starcuk, V. Sklenar, New hard pulse sequence for solvent signal suppression in Fourier transform NMR II. *J. Magn. Reson.* **66,** 391–397 (1986).
21. M. S. Silver, R. I. Joseph, D. I. Hoult, Highly selective $\pi/2$ and π pulse generation. *J. Magn. Reson.* **59,** 347–351 (1984).
22. J. Mao, T. H. Mareci, E. R. Andrew, Experimental study of optimal selective 180° radiofrequency pulses. *J. Magn. Reson.* **79,** 1–10 (1988).
23. A. A. Maudsley, G. B. Matson, J. W. Hugg, M. W. Weiner, Reduced phase encoding in spectroscopic imaging. *Magn. Reson. Med.* **31,** 645–651 (1994).
24. K. L. Behar, T. Ogino, Assignment of resonances in the ^1H spectrum of rat brain by two-dimensional shift correlated and *J*-resolved NMR spectroscopy. *Magn. Reson. Med.* **17,** 285–303 (1991).
25. T. Michaelis, K.-D. Merboldt, W. Hänicke, M. L. Gyngell, H. Bruhn, J. Frahm, On the identification of cerebral metabolites in localized ^1H NMR spectra of human brain *in vivo*. *NMR Biomed.* **4,** 90–98 (1991).
26. D. C. Shungu, J. D. Glickson, Band-selective spin echoes for *in vivo* localized ^1H NMR spectroscopy. *Magn. Reson. Med.* **32,** 277–284 (1994).
27. M. L. Gyngell, T. Els, M. Hoehn-Berlage, K.-A. Hossmann, Localised 1H MRS of experimental brain tumours in rats *in vivo*, *in* "Proc., SMRM, 12th Annual Meeting, New York, 1993," p. 14.